



# Pelagic production and the recruitment of juvenile polar cod *Boreogadus saida* in Canadian Arctic seas

Mathieu LeBlanc<sup>1</sup> · Maxime Geoffroy<sup>2</sup> · Caroline Bouchard<sup>3</sup> · Stéphane Gauthier<sup>4</sup> · Andrew Majewski<sup>5</sup> · James D. Reist<sup>5</sup> · Louis Fortier<sup>1</sup>

Received: 20 December 2018 / Revised: 21 August 2019 / Accepted: 23 August 2019 / Published online: 5 September 2019  
© The Author(s) 2019

## Abstract

Previous work found that an earlier ice breakup favors the recruitment of juvenile polar cod (*Boreogadus saida*) by enabling early hatchers to survive and reach a large size by late summer thanks to a long growth season. We tested the hypothesis that, in addition to a long growth season, an earlier ice breakup provides superior feeding conditions for young polar cod by enhancing microalgal and zooplankton production over the summer months. Ice cover and surface chlorophyll *a* were derived from satellite observations, and zooplankton and juvenile cod biomass were estimated by hydroacoustics in ten regions of the Canadian Arctic over a period of 11 years. Earlier breakups resulted in earlier phytoplankton blooms. Zooplankton backscatter in August increased with earlier breakup and bloom, and plateaued at chlorophyll *a* > 1 mg m<sup>-3</sup>. Juvenile cod biomass in August increased with an earlier breakup, and plateaued at a zooplankton backscatter > 5 m<sup>2</sup> nmi<sup>-2</sup>, supporting the hypothesis that higher food availability promotes the growth and survival of age-0 fish in years of early ice melt. However, there was little evidence that late summer biomass of either zooplankton or age-0 polar cod benefitted from ice breakup occurring prior to June. On average, zooplankton standing stock was similar in the Southern Beaufort Sea and the North Water-Lancaster Sound polynya complex, but juvenile cod biomass was higher in the Beaufort Sea. Intense avian predation could explain the lower biomass of juvenile cod in the polynya complex, confirming its reputation as a biological hotspot for energy transfer to higher trophic levels.

**Keywords** *Boreogadus saida* · Juvenile recruitment · Zooplankton · Ice breakup date · Phytoplankton bloom · Canadian Arctic Ocean

---

This article belongs to the special issue on the "Arctic Gadids in a Changing Climate", coordinated by Franz Mueter, Haakon Hop, Benjamin Laurel, Caroline Bouchard, and Brenda Norcross.

---

**Electronic supplementary material** The online version of this article (<https://doi.org/10.1007/s00300-019-02565-6>) contains supplementary material, which is available to authorized users.

---

✉ Mathieu LeBlanc  
mathieu.leblanc.10@ulaval.ca

<sup>1</sup> Québec-Océan, Department of Biology, Université Laval, Québec, QC G1V 0A6, Canada

<sup>2</sup> Centre for Fisheries Ecosystems Research, Marine Institute of Memorial University of Newfoundland, St. John's, NL A1C 5R3, Canada

## Introduction

The polar cod (*Boreogadus saida*), a small forage fish, dominates the pelagic fish assemblage in Arctic seas (Fortier et al. 2015). It plays a pivotal role in the transfer of energy from zooplankton to Arctic predators, thus changes in its abundance in response to climate change could alter the services provided to northern communities by the pelagic ecosystem (Welch et al. 1992; Tynan and DeMaster 1997; Darnis et al. 2012). The larvae hatch from January to early July and develop

<sup>3</sup> Greenland Climate Research Centre, Greenland Institute of Natural Resources, Kivioq 2, 3900 Nuuk, Greenland

<sup>4</sup> Institute of Ocean Sciences, Fisheries and Oceans Canada, Sidney, BC V8L 4B2, Canada

<sup>5</sup> Freshwater Institute, Fisheries and Oceans Canada, Winnipeg, MB R3T 2N6, Canada

in the epipelagic layer (0–100 m) over spring and summer (Bouchard and Fortier 2008, 2011; Geoffroy et al. 2016). By September and October, age-0 juvenile polar cod initiate an ontogenetic downward migration and recruit progressively to the adult stock in the mesopelagic layer as their size increases (Geoffroy et al. 2016). The abundance and biomass of epipelagic age-0 polar cod in August and September, before this migration, is believed to be a predictor of recruitment to the adult population (e.g., polar cod in Bouchard et al. 2017; other gadids in Laurel et al. 2016).

In the Canadian Arctic, the biomass of juvenile polar cod in August and September increases exponentially with earlier ice breakup (< 50% ice cover) and warmer spring–summer sea surface temperatures (Bouchard et al. 2017). Only the late hatchers survive in years of late ice breakup, resulting in fewer and smaller fish in the fall. In years of early ice breakup, early hatchers survive and enjoy a long growth season, which results in more abundant and heavier fish in the fall. Differences in recruitment to the juvenile stage can be large: juvenile polar cod biomass in September can be 11 times greater for an early May ice breakup compared to a late September ice breakup (Bouchard et al. 2017). Juvenile recruitment was strongly correlated to ice breakup date and sea surface temperatures (SST), two correlated abiotic drivers. However, Bouchard et al. (2017) suspected that the survival of early hatchers in years of early ice breakup is enhanced by biotic factors such as an advanced bloom of ice algae and phytoplankton (e.g., Kahru et al. 2011) and the resulting earlier and more intense production of copepod nauplii and copepodites (Fortier et al. 1995; Ringuette et al. 2002; Daase et al. 2013), the preferred prey of age-0 polar cod (Michaud et al. 1996; Bouchard et al. 2016).

In this study, new data are added (18 region-year combinations in August and 12 in September) to further explore the correlation between ice breakup date and the biomass of juvenile polar cod in late summer reported by Bouchard et al. (2017). We also test the prediction that increased juvenile recruitment in years of early ice breakup is correlated to an earlier phytoplankton bloom and the resulting higher availability of zooplankton. Phytoplankton bloom onset date and acoustically estimated zooplankton standing stock in the fall are used as indices of the production of the pelagic ecosystem over the summer months. Pelagic production and the recruitment of juvenile polar cod are contrasted among three provinces of the Canadian Arctic: Southern Beaufort Sea in the Arctic Ocean Basin proper, the shallow Kitikmeot region in the central Archipelago, and Northwest Baffin Bay including the North Water-Lancaster Sound polynya complex.

## Materials and methods

### Study area

The Canadian sector of the Arctic Ocean extends from the Beaufort Sea in the West to Baffin Bay in the East (Fig. 1). The sector is divided into several regions by the Canadian Ice Service based on sea-ice characteristics and regime ([www.ec.gc.ca/glaces-ice](http://www.ec.gc.ca/glaces-ice)). Typically, these regions are covered by ice for most of the year, with ice breakup occurring from May to September or not at all depending on the year (Bouchard et al. 2017; National Snow and Ice Data Center 2018). From 2006 to 2017, 63 hydroacoustic-trawl surveys of variable duration (1 to 30 days) were completed in ten of these regions in August and September (Fig. 1, Table 1) as part of the ArcticNet annual expedition of the research icebreaker CCGS *Amundsen* to the Canadian Arctic Ocean (2006–2017) and the Fisheries and Oceans Canada surveys aboard the trawler F/V *Frosti* in the Beaufort Sea (2012–2014). Overall, valid hydroacoustic estimates of zooplankton and juvenile polar cod biomass were obtained for 40 region-year combinations in August and 23 in September (Table 1).

The ten regions surveyed span three main oceanographic provinces (Fig. 1). Southern Beaufort Sea in the west comprises the productive Mackenzie Shelf with intermittent upwelling at its northeast edge (Carmack and Kulikov 1998; Carmack et al. 2004); the mouth of the Amundsen Gulf with the large Cape Bathurst polynya (Stirling 1980; Arrigo and van Dijken 2004; Williams and Carmack 2008); and the deep Amundsen Gulf. The Kitikmeot region in the Southern Canadian Arctic Archipelago (CAA) is characterized by shallow (< 220 m) gulfs, sounds and straits (Coronation-Queen Maud gulfs, Larsen Sound-Victoria Strait), and deeper (< 420 m) sounds and channels (Peel Sound, M'Clintock Channel). Northwest Baffin Bay includes the productive North Water and Lancaster Sound polynya complex, and the western Baffin Bay region (Fig. 1). The west–east general circulation carries surface waters from the Beaufort Sea to Baffin Bay through the shallow CAA (Wang et al. 2012). Biologically, polar cod and the large copepods *Calanus hyperboreus* and *Calanus glacialis* dominate pelagic biomass in the deep Beaufort Sea and NW Baffin Bay, while benthic fish and smaller copepods characterize the shallow Kitikmeot (Bouchard et al. 2018, Darnis et al. unpublished data). The North Water and Lancaster Sound polynya complex is considered one of the most biologically productive regions of the Arctic Ocean (e.g., Stirling 1980; Barber et al. 2001; Tremblay et al. 2002).

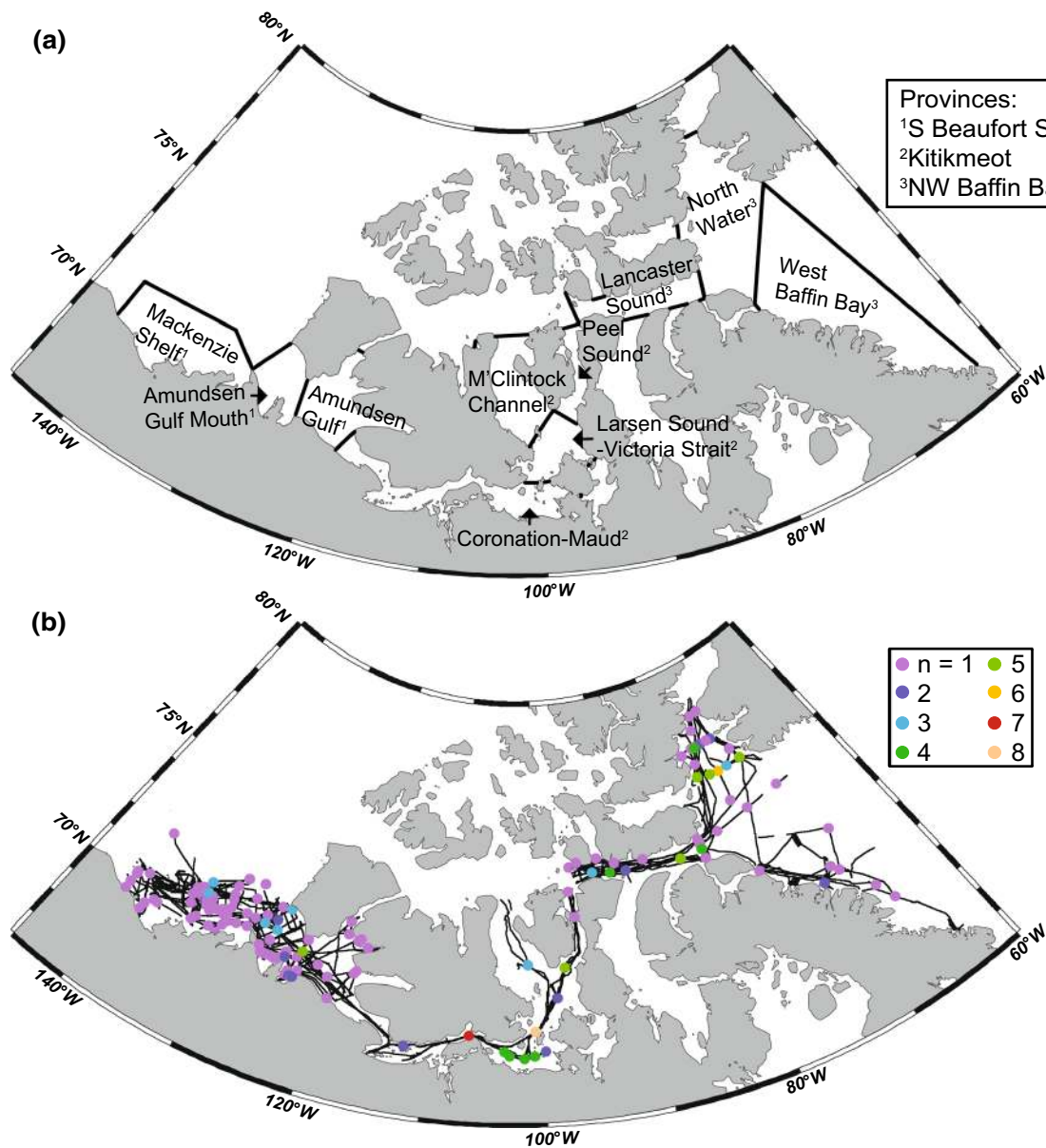


**Fig. 1** **a** Limits of the ten Canadian Ice Service regions analysed in the study grouped by the Southern Beaufort Sea, Kitikmeot and Northwest Baffin Bay oceanographic provinces. **b** Hydroacoustic and ichthyoplankton surveys from 2006 to 2017. Black lines represent

hydroacoustic transects. Colored dots are the locations of ichthyoplankton sampling stations with color indicating the number of net samples at each location over the study period

### Remote sensing of ice and Chl *a*

Ice breakup week (IBW) in a given region-year was defined as the week during which ice concentration fell below 50% (Scott and Marshall 2010) using the Canadian Ice Service data ([www.ec.gc.ca/glaces-ice](http://www.ec.gc.ca/glaces-ice)).

For each region-year, the mean chlorophyll *a* concentration from 1 April to 31 August (Chl *a*) was estimated using Level 3 daily Aqua MODIS remote-sensing data at a 4 km<sup>2</sup> resolution (<https://oceancolor.gsfc.nasa.gov/cgi/l3>).

Daily sea-ice concentration was assigned to each Chl *a* concentration from the nearest most overlapping pixel of the 25-km resolution Defense Meteorological Satellite Program (DMSP) Special Sensor Microwave Imager (SSM/I)-Special Sensor Microwave Imager/Sounder (SSMIS) (<https://nsidc.org>, 2006–2016) and of the 12.5-km resolution IFREMER-CERSAT (<ftp.ifremer.fr/ifremer/cersat> 2017) datasets. Pixels of Chl *a* concentration with ice concentration > 15% were removed from the analysis to avoid possible contamination of the ocean color signal. For a given region-year, the

**Table 1** Date range of ichthyoplankton and hydroacoustic sampling periods in each region: Southern Beaufort Sea: *MS* Mackenzie Shelf, *AGM* Amundsen Gulf Mouth, *AG* Amundsen Gulf; Kitikmeot: *CM* Coronation-Maud, *LV* Larsen Sound-Victoria Strait, *MC* M'Clintock Channel, *PS* Peel Sound; and Northwest Baffin Bay: *LS* Lancaster Sound, *NW* North Water, *WBB* West Baffin Bay

Month	Year	MS	AGM	AG	CM	LV	MC	PS	LS	NW	WBB	
August	2010	14–28				9–10		8–9	6–8			
	2011				9–12	8–9		7–8	2–7			
	2012	6–31										
	2013	24–31	1–24	10–20					13–31	14–29	9–12	
	2014	2–31	17–21		11–16			10–11		1–7		
	2015	25–30	22–30	22	17–21	17		16–17	9–14		5–9	
	2016	29–31	27–29	26–27	20–26	19–20		19	4–18	4–17	1–3	
	2017				8–10	7–10			2–5			
	September	2006				24–27		23–24		6–23	6–20	
		2007									28–30	
2008									2–9	9–23	10–30	
2011		2–30	1–30									
2013									3–29			
2014		1–24		24–25								
2015					19–22	22–23			25–30			
2016		1–6		15–16	16–20	20	21–22		23–25		26–29	

No sampling in 2009

phytoplankton bloom start date (BSD) was defined as the day when the daily mean Chl *a* concentration exceeded 20% of the maximum daily mean Chl *a* concentration from 1 April to 31 August (Platt et al. 2009; Marchese et al. 2017).

### Hydroacoustic estimates of polar cod and zooplankton

Ichthyoplankton nets and trawls were deployed (Fig. 1b, Table 1) from the surface to depths varying from 10 to 100 m to ascertain the epipelagic fish assemblage and validate the acoustic signals (details in Bouchard et al. 2017). The fresh standard length (SL) of individual age-0 polar cod was measured on the ship and their weight (W) was calculated based on  $W = 0.0055 (SL)^{3.19}$  (Geoffroy et al. 2016). Data from the two ships for a given region-year were pooled.

Hydroacoustic data were recorded continuously along the track of the ships (Fig. 1b, Table 1) with a Simrad EK60@ split-beam echosounder at 38 and 120 kHz (nominal beam angle of 7°). The ping rate varied from ~1 to 2 s depending on maximum depth, and pulse duration was set to 1024 μs. Power was 2 kW at 38 kHz and 500 W (2006–2011) or 250 W (2012–2017) at 120 kHz. The co-located transducers were calibrated annually using the standard sphere method (Demer et al. 2015). Conductivity–Temperature–Depth (CTD) profiles from the *Amundsen* (SBE-911 plus®) and the *Frosti* (SBE-25® and SBE-19 plus V2®) were used to determine sound speed in water (Mackenzie 1981) and the coefficient of sound absorption (Francois and Garrison 1982) for the acoustic analysis. The echograms were all scrutinized to correct bottom detection by the sounder and to discard noise and signals from other deployed instruments. A time-varied

threshold ( $TVT = 20 \log R + 2\alpha R - 140$ , where *R* is the range from the transducer) was also added in the 38 and 120 kHz echograms to offset noise amplification at depth by the time-varied gain (e.g., Geoffroy et al. 2016). A minimum (−90 dB) and a maximum (−40 dB) volume backscattering strength ( $S_v$ ; dB re:  $1 \text{ m}^{-1}$ ) threshold was applied on the data at both frequencies (Benoit et al. 2014; Geoffroy et al. 2016).

The difference in mean volume backscattering strength  $\Delta MVBS$  (dB re:  $1 \text{ m}^{-1}$ ) between 38 and 120 kHz was used to discriminate polar cod from zooplankton ( $\Delta MVBS_{120-38}$  in the range −10 dB to 5 dB, Benoit et al. 2014; Geoffroy et al. 2016). Monthly mean size (SL and W) of polar cod sampled by nets and the nautical area backscattering coefficient (NASC,  $\text{m}^2 \text{ nmi}^{-2}$ ) in echo-integration cells (0.25 nautical mile long by 3 m deep) at 38 kHz were used to estimate age-0 polar cod integrated biomass ( $\text{mg m}^{-2}$ ) from 13.5 m (effective sampling depth of the transducers) to 100 m. Monthly (August and September) mean integrated age-0 polar cod biomass (B) was calculated for each region-year surveyed (Table 1).

By excluding fish in the top 13.5 m of the water column and at the ice-water interface, our acoustical estimates of age-0 polar cod biomass are underestimating total biomass. The proportion of the age-0 population excluded from the estimates is poorly documented, but the bias is assumed constant across years and regions.

A proxy for zooplankton density in the epipelagic layer (13.5–100 m) was calculated using NASC ( $\text{m}^2 \text{ nmi}^{-2}$ ) in echo-integration cells at 120 kHz. To discriminate zooplankton backscatter from that of fish and macrozooplankton, only cells with  $\Delta MVBS_{120-38} > 12$  dB (Madureira et al. 1993) were kept in the echo-integration.

Monthly mean zooplankton backscatter (Zoo) was calculated for each region-year.

Copepods dominate the zooplankton of Canadian Arctic seas with the large *Calanus hyperboreus* and *C. glacialis* herbivores making up 50 to 90% of the zooplankton biomass and small species such as *Pseudocalanus* spp., *Oithona similis*, and *Triconia borealis* prevailing by numbers (Darnis et al. 2008, 2012). We thus assumed that the acoustic signal attributed to zooplankton is dominated by these species.

All hydroacoustic data analyses were performed with Echoview® 7.1.

## Statistics

Spearman's rank correlations were first tested between abiotic and biotic variables and among biotic variables as exploratory analyses. Each relationship was further investigated using simple linear mixed-effects regression models. In models that included Chl *a* or zooplankton backscatter as independent variables, these variables were ln-transformed based on a visual examination of scatterplots, as well as on the theory of predator–prey interactions (Holling 1959). Region of sampling was included in the models as a random effect. Relationships between zooplankton backscatter or age-0 polar cod biomass and ice breakup week or phytoplankton bloom start date were also evaluated using second-order mixed-effects models. Linear and second-order mixed-effects models were compared with the Akaike information criteria (AIC). Marginal  $r^2$  was calculated for each model (Nakagawa and Schielzeth 2013). Dependent variables in the relationships were ln-transformed prior to statistical analyses to achieve approximate homoscedasticity and normality of model residuals.

Average onset date of the phytoplankton bloom, zooplankton backscatter in August, and age-0 polar cod biomass in August were compared among oceanographic provinces with a one-way ANOVA and a Tukey HSD test.

Statistical analyses were conducted with R® version 3.2.3 (R Core Team 2015).

## Results

### Ice breakup, microalgal bloom, zooplankton and juvenile polar cod biomass

Across the region-years, the onset date of the phytoplankton bloom was significantly influenced (slope = 0.020,  $p = 0.002$ ) by the ice breakup week (linear mixed-effects model, Fig. 2a; Online resource 1a). Chl *a* averaged over the period 1 April to 31 August was significantly correlated to ice breakup week (Spearman's rank correlation,  $p < 0.001$ ), although the effect was not statistically significant in the

linear mixed-effects model (slope =  $-0.018$ ,  $p = 0.108$ ). Earlier ice breakup tended to result in greater surface microalgal biomass over spring–summer (Fig. 2b; Online resource 1b).

Based on the linear mixed-effects model, zooplankton backscatter in the epipelagic layer (13.5–100 m) in August increased with an earlier ice breakup week (slope =  $-0.170$ ,  $p < 0.001$ ) and an earlier phytoplankton bloom (slope =  $-0.015$ ,  $p = 0.014$ ) (Fig. 3a, b; Online resource 2a). An early ice breakup in May increased zooplankton backscatter up to 116-fold relative to a late ice breakup in September (Fig. 3a). A second-order mixed-effects model [ $\ln(\text{Zoo}) = 1.11 - 4.92 \text{ IBW} - 2.89 \text{ IBW}^2$ ] yielded a higher coefficient of determination (marginal  $r^2 = 0.51$  vs. 0.36) and a lower AIC value (110.8 vs. 118.7) than did the linear mixed-effects model (Fig. 3a), suggesting that zooplankton backscatter was maximum for an ice breakup in early June. Based on a second-order mixed-effects model as well (marginal  $r^2 = 0.23$  vs. 0.17; AIC value = 122.5 vs. 124.4), zooplankton backscatter peaked when the surface bloom started in late May (Fig. 3b). Despite much noise in the relationship, zooplankton backscatter in late summer tended to increase initially with spring–summer Chl *a* (slope = 0.453,  $p = 0.363$ ), and then to plateau at Chl *a*  $> 1 \text{ mg m}^{-3}$  (Fig. 3c).

Biomass of age-0 polar cod ( $\text{mg m}^{-2}$ ) in August in the epipelagic layer increased with an earlier ice breakup (slope =  $-0.254$ ,  $p < 0.001$ ) (Fig. 4a; Online resource 3a). Polar cod biomass in August was ~16 times higher for the earliest ice breakup on week 19 (early May) compared to the latest ice breakup on week 36 (early September). As for zooplankton backscatter, the residuals of the linear mixed-effects regression tended to be positive in June and negative before and after, suggesting that juvenile polar cod biomass in August was maximum when the ice broke up in June. A second-order mixed-effects model also yielded a slightly higher coefficient of determination (marginal  $r^2 = 0.47$  vs. 0.44) and a lower AIC value (135.6 vs. 142.6) than did the linear mixed-effects model (Fig. 4a). Age-0 polar cod biomass in August increased with zooplankton backscatter (slope = 0.762,  $p < 0.001$ ) until it reached a plateau at zooplankton backscatter  $> 5 \text{ m}^2 \text{ nmi}^{-2}$  (Fig. 4b).

The relationships found in August between abiotic and biotic variables and among biotic variables were also detected in September but at lower statistical significance levels (Online Resources 2 to 5).

### Bloom onset date, zooplankton standing stock and juvenile polar cod biomass across oceanographic provinces

The onset date of the phytoplankton bloom averaged over years tended to be more variable in regions of the Southern Beaufort Sea than in the regions of the other two

**Fig. 2** **a** Bloom start day (BSD) and **b** average surface chlorophyll *a* concentration from 1 April to 31 August (Chl *a*) in relation to ice breakup week (IBW) for all region-years (filled symbols: August; open symbols: September;  $n=52$ ) over the period of study. Solid lines are the linear mixed-effects regression models and dashed lines are the 95% confidence intervals. Regression equations are given with the  $p$  value of the slope and marginal  $r^2$ .  $\rho$  is the Spearman's rank correlation

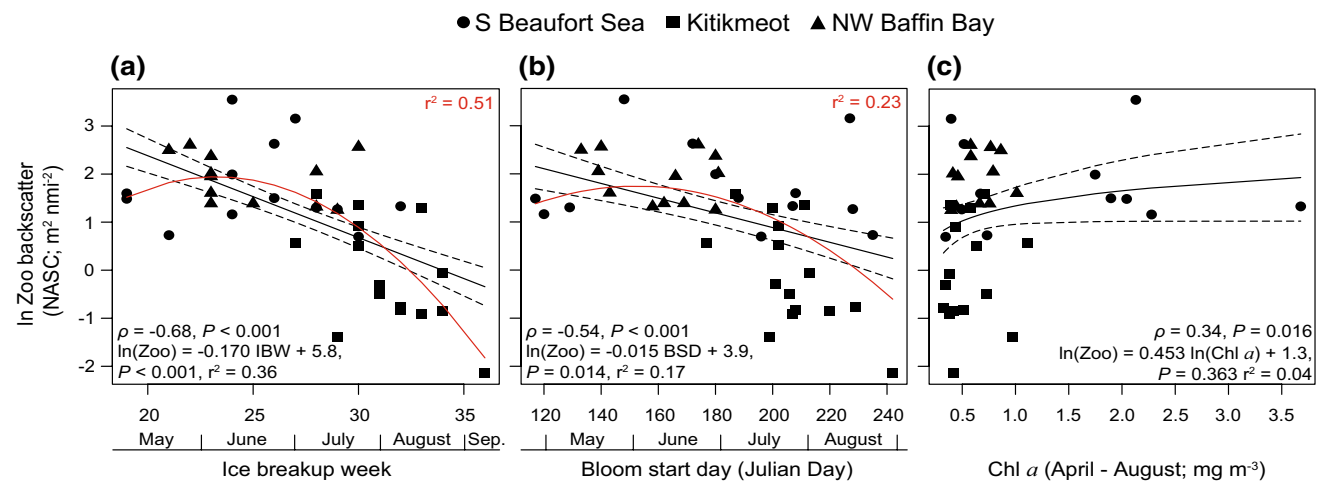
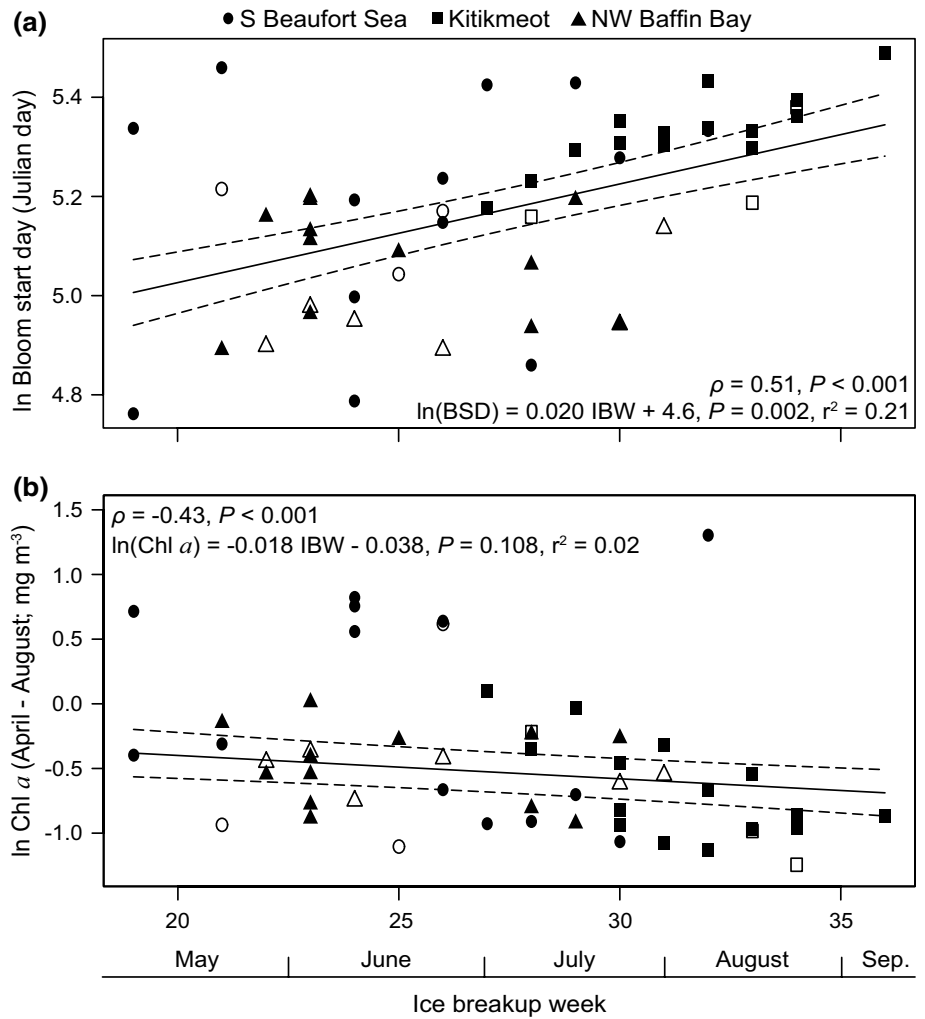


**Fig. 3** Mean epipelagic zooplankton backscatter (Zoo) in August ( $n=40$ ) in relation to **a** ice breakup week (IBW), **b** bloom start day (BSD), and **c** mean surface chlorophyll *a* concentration from 1 April to 31 August (Chl *a*). Solid black lines are the (a, b) linear or c logarithmic mixed-effects regression models and dashed lines are the 95%

confidence intervals. Regression equations are given with the  $p$  value of the slope and marginal  $r^2$ .  $\rho$  is the Spearman's rank correlation. Red curves (a, b) are second-order mixed-effects regression models fitted to the data (see Results)

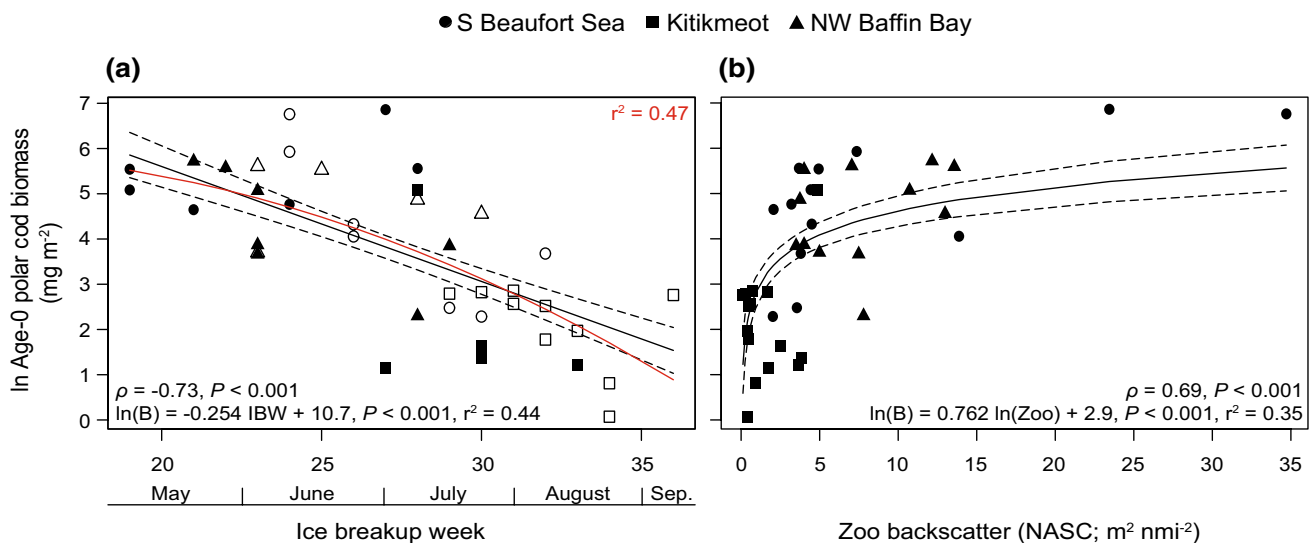


**Fig. 4** Mean epipelagic age-0 polar cod biomass (B) in August ( $n=40$ ) in relation to **a** ice breakup week (IBW), and **b** mean epipelagic zooplankton backscatter (Zoo) in August. Solid lines are the **a** linear or **b** logarithmic mixed-effects regression models and dashed lines are the 95% confidence intervals. Regression equations are

given with the  $p$  value of the slope and marginal  $r^2$ .  $\rho$  is the Spearman's rank correlation. Red curve **a** is a second-order mixed-effects regression model fitted to the data (see Results). Open symbols represent data presented in Bouchard et al. (2017)

oceanographic provinces (Fig. 5a). Bloom start dates were significantly later (Tukey HSD test,  $p < 0.05$ ) in the Kitikmeot province of the Canadian Archipelago, and showed no statistical difference between the Southern Beaufort Sea and NW Baffin Bay.

Mean acoustic estimates of zooplankton density in August were similar in the deep Southern Beaufort Sea and deep NW Baffin Bay and significantly lower (Tukey HSD test,  $p < 0.05$ ) in the shallow Kitikmeot (Fig. 5b).

Juvenile polar cod biomass in August averaged over region-years was highest in Southern Beaufort Sea (mean =  $252 \text{ mg m}^{-2}$ ), intermediate in NW Baffin Bay (mean =  $139 \text{ mg m}^{-2}$ ) and lowest in the Kitikmeot (mean =  $19 \text{ mg m}^{-2}$ ) (Fig. 5c).

## Discussion

### Early ice breakup and summer pelagic production

In the strongly pulsed primary production cycle of Arctic seas, microalgal biomass first develops in spring at the ice-water interface (Horner 1985; Sakshaug and Slagstad 1991; Søreide et al. 2010). Thanks to early removal of the snow cover over the ice or to leads allowing light to penetrate the surface waters, phytoplankton sometimes blooms before the ice breakup (Haecy et al. 1998; Fortier et al. 2002; Arrigo et al. 2012; Assmy et al. 2017). However, the surface phytoplankton bloom typically starts in the weeks following ice breakup and then deepens towards the nitracline to

form a sub-surface chlorophyll maximum (SCM) (Martin et al. 2010). With an increasingly late freeze-up allowing wind mixing, a second surface phytoplankton bloom is now observed in autumn in many Arctic seas (Ardyna et al. 2014).

By allowing light penetration, an earlier ice breakup triggers an earlier phytoplankton bloom (e.g., Ringuette et al. 2002; Kahru et al. 2011; Leu et al. 2011), which results in a longer season of production and, despite the possibility of nutrients becoming limiting in some regions (Tremblay et al. 2012), an overall greater primary production over the spring–summer (Arrigo et al. 2008; Arrigo and van Dijken 2015). Satellite observations detect neither ice microalgae, under-ice phytoplankton, nor deep SCMs (Arrigo and van Dijken 2015). Hence, the remote-sensing measurements of surface Chl  $a$  used here certainly underestimated the overall microalgal biomass available to zooplankton grazers over spring–summer (e.g., Assmy et al. 2017). Nevertheless, surface Chl  $a$  averaged from April to August, our crude index of ecosystem primary production, was correlated to ice breakup week (Fig. 2). Bloom start date, which dictates the duration of the period of food availability to zooplankton grazers, also depended on ice breakup week as reported previously (e.g., Ringuette et al. 2002; Søreide et al. 2010; Leu et al. 2011).

First-feeding polar cod larvae prey on copepod eggs and the naupliar stages of small copepods such as *Pseudocalanus* spp. and *Oithona similis*, whereas juveniles shift their diet to the nauplii and early copepodite stages of the larger *Calanus* spp. (Fortier et al. 1995; Michaud et al. 1996; Bouchard et al. 2016). An early ice breakup in the North Water relative to

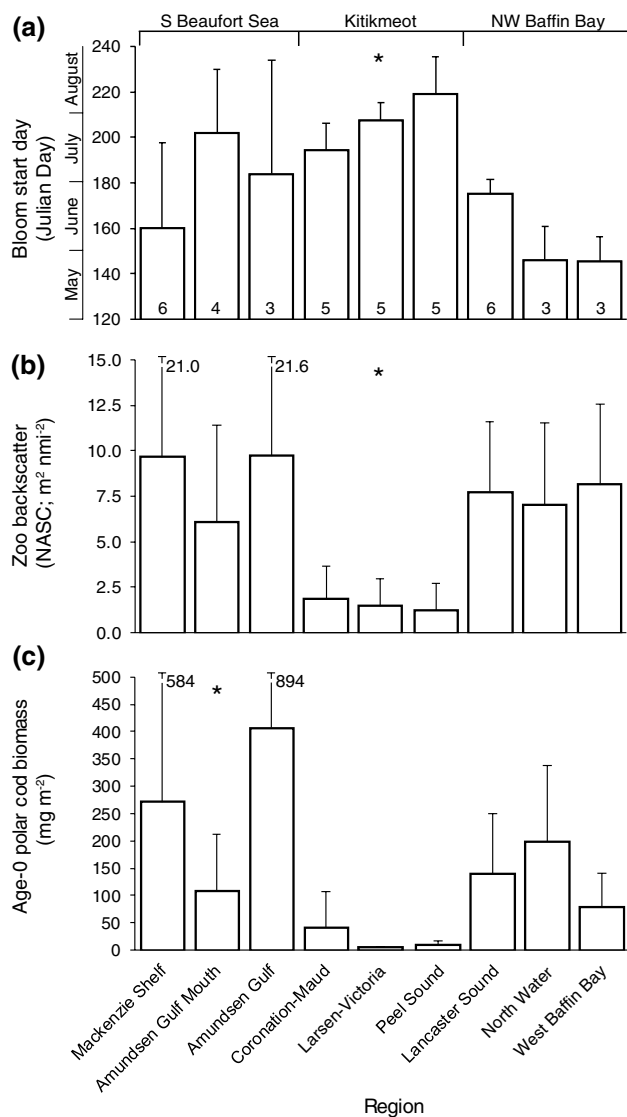


**Fig. 5** Mean values over the study period of **a** bloom start day, **b** epipelagic zooplankton backscatter in August, and **c** epipelagic age-0 polar cod biomass in August, for different regions of the Canadian Arctic grouped by oceanographic provinces. Number of years analysed over the study period is indicated in bars of panel (a). No values were measured in August in M'Clintock Channel. Oceanographic province with significantly different values based on one-way ANOVA and Tukey HSD test ( $p < 0.05$ ) is represented by an asterisk

Barrow Strait led to the earlier production and higher densities of *Pseudocalanus* spp. and *Calanus* spp. early copepodite stages (Ringuette et al. 2002). As well, Leu et al. (2011) observed a temporal mismatch between the algal bloom and the growth of the new copepod generation when ice broke up late in Rijpfjorden (Svalbard) in 2008. These authors suggested that very early ice breakups and algal blooms could also disconnect herbivorous zooplankton from its food, leading to lower population levels, as has been also observed at lower latitudes in the Bering Sea (Hunt et al. 2002).

In the present study, zooplankton backscatter in August was more strongly correlated to ice breakup date and phytoplankton bloom onset date than to Chl *a* concentration (Fig. 3), indicating that the duration of the season of food availability rather than food abundance likely was the primary driver of the late summer biomass of zooplankton. Over a 4-month range in ice breakup and phytoplankton bloom dates (early May to early September), zooplankton backscatter in August generally increased with an earlier breakup and bloom (Fig. 3). Yet, a close inspection of the relationship reveals that maximum backscatter in August was achieved for ice breakups and blooms occurring in late May and June and that, consistent with the prediction of Leu et al. (2011), the few instances of very early breakup and bloom in May were correlated with somewhat lower zooplankton backscatter in August (Fig. 3a, b). Statistically, the adjustment of a second-order mixed-effects model depicting this maximum in zooplankton recruitment for late May–June breakups and blooms explained a larger fraction of the variance ( $r^2$ ) in zooplankton backscatter in August and resulted in a better model (lower AIC) than a linear mixed-effects model (Fig. 3a, b). Maximum zooplankton backscatter would point to June as the threshold over which climate warming and an ever earlier ice breakup would stop benefiting the present zooplankton assemblage in Arctic seas.

### Pelagic production and juvenile polar cod recruitment

Statistical relationships linking fish recruitment to some environmental factor often fail with the addition of new observations, in particular if these come from outside the range of conditions for which the initial relationship was established (Frank 1997; Myers 1998; Leggett and Frank 2008). The addition of 18 new data points for August (from 22 to 40) to the relationship reported by Bouchard et al. (2017) confirmed the link between juvenile polar cod biomass in the fall and the date of ice breakup (Fig. 4a). This suggests that the environmental conditions in Canadian Arctic seas have not yet changed enough to modify the forcing of polar cod recruitment by sea-ice dynamics.

Polar cod is often associated with the ice-water interface and sometimes observed within anfractuosités in the sea ice (Lønne and Gulliksen 1989; Gradinger and Bluhm 2004; Søreide et al. 2006; Melnikov and Chernova 2013; David et al. 2016). This raises the possibility that in region-years of late ice breakup, some age-0 polar cod would ascend to the ice-water interface in August–September, escaping detection in the 13.5 + m layer ensonified by our echosounder. The concentration of juvenile polar cod at the ice-water interface or within the top 13.5 m of the water column could explain in part the estimated low biomasses of age-0 fish in years of late breakup. In the central Arctic Ocean, polar cod sampled



at the ice–water interface with the Surface and Under Ice Trawl (SUIT) in August and September were age-1 + fish from 52 to 140 mm SL (David et al. 2016). The 0.3 mm mesh of the inside net of the SUIT should have retained age-0 polar cod if any were distributed at the ice-water interface. Other studies also reported that polar cod associated with sea ice were mostly age-1 and age-2 fish (Lønne and Gulliksen 1989; Melnikov and Chernova 2013). While further studies of sea ice as habitat for age-0 polar cod are warranted (Geoffroy et al. 2016), these observations do not support the hypothesis of a significant migration of age-0 polar cod to the ice–water interface in the fall.

The dependence of juvenile polar cod biomass on ice breakup date can be interpreted in two non-exclusive ways (Bouchard et al. 2017). First, polar cod larvae hatch from as early as January to the first weeks of July (Bouchard and Fortier 2008, 2011). Higher recruitment in late summer could solely result from the fact that an early ice breakup provides early hatching larvae with the minimum temperature and feeding conditions to survive and benefit from a long growth season, leading to abundant and large fish in August. Warmer summer temperatures and more abundant food would play no significant role in polar cod survival and recruitment. Second, in addition to minimum conditions for survival, warmer SST and a general increase in summer pelagic production resulting from an earlier bloom would also contribute to maximize juvenile polar cod biomass in late summer in region-years of early ice breakup. It is difficult to tease apart the respective roles of early breakup and high SST as they are highly correlated (Bouchard et al. 2017). In the laboratory, age-0 polar cod achieved better morphometric and lipid conditions at high temperature (5° vs. 2 °C) or high food ration (2–5 vs. 0.5 prey ml<sup>-1</sup>) (Koenker et al. 2018). The present field study confirms that the zooplankton food available to young polar cod increases with an earlier ice breakup and phytoplankton bloom onset (Fig. 3a, b); and that the biomass of juvenile polar cod in August is limited at low densities of zooplankton (Fig. 4b). The dependence of polar cod recruitment on zooplankton density followed the expected asymptotic curve predicted by theory when predators become saturated beyond some threshold prey concentration (Holling 1959; Cushing and Horwood 1994). Therefore, the emerging proximal mechanism behind the enhancement of juvenile polar cod recruitment with early ice breakup is the maximization of pre-winter sizes, and possibly lipid storage, by exposing early hatchlings to higher SST and saturating feeding conditions.

Bouchard et al. (2017) reported weaker relationships between epipelagic juvenile polar cod biomass and ice breakup date or spring–summer SST for acoustic surveys conducted in October relative to August or September. They attributed the seasonal deterioration of the relationships to the downward migration of the juveniles leaving

the epipelagic layer (Geoffroy et al. 2016), and emphasized the importance of conducting surveys during the appropriate temporal window (Bouchard et al. 2017). In the present study, all relationships involving the backscatter of zooplankton were weaker in September than in August (Online resource 2 to 5). By September, the *Calanus* species making up the bulk of zooplankton biomass have initiated or completed their seasonal vertical migration to depths > 100 m (Dawson 1978; Hirche 1997; Darnis and Fortier 2014). Moreover, an earlier ice breakup and phytoplankton bloom accelerate the development of Arctic copepods and hasten their migration to depth (e.g., Ringuette et al. 2002). While the backscatter of larger macro-zooplankton was excluded in our acoustic analyses, zooplankton backscatter recorded at 120 kHz might have included that of other organisms similar in size to large copepods (e.g., small amphipods). Notwithstanding this potential bias, our results suggest that August is the optimal time window for acoustic surveys aiming at capturing the dependence of juvenile polar cod recruitment on the availability of their epipelagic copepod prey.

Extrapolating the ongoing trend in earlier ice breakup in the different regions studied, Bouchard et al. (2017) projected some admittedly unrealistic increases in the biomass of polar cod by mid-century. They concluded that several factors amplified by the ongoing warming of the Arctic would likely limit an eventual proliferation of polar cod, including the reduction in habitat for the ice-associated individuals and the invasion of Arctic seas by competing or predatory subarctic fish species. In the present study, both the backscatter of zooplankton (Fig. 3a) and biomass of juvenile polar cod (Fig. 4a) were maximum for ice breakups occurring from late May to early July and tended to stagnate or decline for earlier ice breakups in May (note the log scales in both Figs. 3, 4). This parallel response suggests that a mismatch between copepods and their food when the ice breaks earlier than June (Leu et al. 2011) could cascade to the recruitment of juvenile polar cod and contribute to limit the population development of this key species in response to climate warming.

### Contrasting oceanographic provinces: depth, seabirds, and the recruitment of polar cod

The Southern Beaufort Sea and the NW Baffin Bay oceanographic provinces are characterized by deep regions and the presence of a large recurrent polynyas (respectively the Cape Bathurst polynya and the North Water-Lancaster Sound polynya complex). The North Water-Lancaster Sound polynya complex in particular is considered an oasis for Arctic predators (Stirling 1980; Brown and Nettleship 1981; Heide-Jørgensen et al. 2013). By contrast, shallow depths (< 100 m) and the resulting absence of warm Atlantic Water limit the abundance of large *Calanus* copepods and adult polar cod

in the Kitikmeot (Bouchard et al. 2018; Darnis et al. unpublished data). Over the period covered by the present study (2006–2017), ice breakups in the regions of the Kitikmeot were among the latest and ranged between early July and early September. Unsurprisingly, the average onset date of the phytoplankton bloom was significantly later (Tukey HSD test,  $p < 0.05$ ) in this province (Fig. 5a).

Similar to the onset date of the bloom, mean zooplankton backscatter in August presented a clear pattern across the three provinces, with high and similar average values in the deep Southern Beaufort Sea and the deep NW Baffin Bay ( $6.1\text{--}9.7\text{ m}^2\text{ nmi}^{-2}$  across regions), and low values ( $< 2\text{ m}^2\text{ nmi}^{-2}$ ) in the shallow Kitikmeot (Fig. 5b). Late ice breakup and phytoplankton bloom, the low abundance of zooplankton prey, and a scarcity of adult polar cod (Bouchard et al. 2018) likely resulted in low juvenile polar cod biomass in the Kitikmeot (Fig. 5c).

In all regions of the Southern Beaufort Sea and the NW Baffin Bay oceanographic provinces, mean zooplankton backscatter exceeded the  $5\text{ m}^2\text{ nmi}^{-2}$  threshold (Fig. 5b) under which juvenile polar cod recruitment seems limited (Fig. 4b). Interestingly, despite non-limiting prey density in both provinces, generally higher mean and maximum juvenile polar cod biomasses were observed in the Southern Beaufort Sea than in NW Baffin Bay (Fig. 5c). Mostly because of the availability of nesting cliffs (Gaston et al. 2012), piscivorous seabirds including the thick-billed murre (*Uria lomvia*), northern fulmar (*Fulmarus glacialis*) and black-legged kittiwake (*Rissa tridactyla*), are considerably more abundant in the North Water-Lancaster Sound polynya complex of NW Baffin Bay than in the Southern Beaufort Sea (Wong et al. 2014). The availability of zooplankton prey being non-limiting in the two provinces, we suspect that intense avian predation lowered juvenile polar cod biomass in NW Baffin Bay relative to the Southern Beaufort Sea (top-down instead of bottom-up control). While energy transfer from lower trophic levels to fish and marine mammals through polar cod could be similar in the two provinces, we suggest that intense avian predation on juvenile polar cod in the North Water-Lancaster Sound polynya complex increases overall energy transfer to higher trophic levels. Our results quantitatively confirm the reputation of the North Water as a biological hotspot, further justifying the transformation of the Pikiyasorsuaq region into an international protected area under Inuit management (see Eegeesiak et al. 2017).

**Acknowledgements** We thank the officers and crew of the CCGS *Amundsen* and *F/N Frosti* for their dedication and professionalism. We are grateful to the several technicians and colleagues who contributed to sampling and analysis over the years. The National Oceanic and Atmospheric Administration graciously lent the transducers used on board the *Frosti*, and Yvan Simard (Fisheries and Oceans Canada) lent the transceivers. Experts at the Canada Excellence Research Chair on

remote sensing of Canada's new Arctic frontier provided the MODIS data and valuable recommendations for their processing. We would also like to thank Franz Mueter, Hauke Flores and two anonymous reviewers for their comprehensive and highly constructive comments. Thanks to the Beaufort Region Environmental Assessment (BREA) program of Indian and Northern Affairs Canada, the Network of Centres of Excellence ArcticNet, the Canadian International Polar Year, and the Canada Foundation for Innovation (Amundsen Science) for financial support. ML received scholarships from the Natural Sciences and Engineering Research Council of Canada (NSERC). This is a contribution to Québec-Océan at Université Laval, ArcticNet, and the Canada Research Chair on the response of Arctic marine ecosystems to climate warming.

**Data availability** Hydroacoustic data collected onboard the CCGS *Amundsen* are available at <https://www.polardata.ca> (CCIN Reference No.: 12841).

## Compliance with ethical standards

**Conflict of interest** The authors declare that they have no conflict of interest.

**Ethical approval** All applicable international, national, and/or institutional guidelines for the care and use of animals were followed. Research licenses obtained since 2014 for ArcticNet annual expeditions onboard the CCGS *Amundsen* are listed at <https://www.arcticnet.ulaval.ca/research/expedition2018.php>.

**Open Access** This article is distributed under the terms of the Creative Commons Attribution 4.0 International License (<http://creativecommons.org/licenses/by/4.0/>), which permits unrestricted use, distribution, and reproduction in any medium, provided you give appropriate credit to the original author(s) and the source, provide a link to the Creative Commons license, and indicate if changes were made.

## References

- Ardyna M, Babin M, Gosselin M, Devred E, Rainville L, Tremblay JE (2014) Recent Arctic Ocean sea ice loss triggers novel fall phytoplankton blooms. *Geophys Res Lett* 41:6207–6212
- Arrigo KR, Perovich DK, Pickart RS, Brown ZW, van Dijken GL, Lowry KE, Mills MM et al (2012) Massive phytoplankton blooms under Arctic Sea ice. *Science* 336:1408–1408
- Arrigo KR, van Dijken GL (2004) Annual cycles of sea ice and phytoplankton in Cape Bathurst polynya, southeastern Beaufort Sea, Canadian Arctic. *Geophys Res Lett* 31:L08304
- Arrigo KR, van Dijken GL (2015) Continued increases in Arctic Ocean primary production. *Prog Oceanogr* 136:60–70
- Arrigo KR, van Dijken GL, Pabi S (2008) Impact of a shrinking Arctic ice cover on marine primary production. *Geophys Res Lett* 35:L19603
- Assmy P, Fernandez-Mendez M et al (2017) Leads in Arctic pack ice enable early phytoplankton blooms below snow-covered sea ice. *Sci Rep* 7:40850
- Barber D, Marsden R, Minnett P, Ingram G, Fortier L (2001) Physical processes within the North Water (NOW) Polynya. *Atmos-Ocean* 39:163–166
- Benoit D, Simard Y, Fortier L (2014) Pre-winter distribution and habitat characteristics of polar cod (*Boreogadus saida*) in southeastern Beaufort Sea. *Polar Biol* 37:149–163

- Bouchard C, Fortier L (2008) Effects of polynyas on the hatching season, early growth and survival of polar cod *Boreogadus saida* in the Laptev Sea. *Mar Ecol Prog Ser* 355:247–256
- Bouchard C, Fortier L (2011) Circum-arctic comparison of the hatching season of polar cod *Boreogadus saida*: a test of the freshwater winter refuge hypothesis. *Prog Oceanogr* 90:105–116
- Bouchard C, Mollard S, Suzuki K, Robert D, Fortier L (2016) Contrasting the early life histories of sympatric Arctic gadids *Boreogadus saida* and *Arctogadus glacialis* in the Canadian Beaufort Sea. *Polar Biol* 39:1005–1022
- Bouchard C, Geoffroy M, LeBlanc M, Majewski A, Gauthier S, Walkusz W, Reist JD et al (2017) Climate warming enhances polar cod recruitment, at least transiently. *Prog Oceanogr* 156:121–129
- Bouchard C, Geoffroy M, LeBlanc M, Fortier L (2018) Larval and adult fish assemblages along the Northwest Passage: the shallow Kitikmeot and the ice-covered Parry Channel as potential barriers to dispersal. *Arctic Sci* 4:781–793
- Brown RGB, Nettleship DN (1981) The biological significance of polynyas to Arctic colonial seabirds. In: Stirling I, Cleator H (Eds.) Polynyas in the Canadian Arctic. Occasional Paper 45. Canadian Wildlife Service, Ottawa, pp 59–66
- Carmack EC, Kulikov EA (1998) Wind-forced upwelling and internal Kelvin wave generation in Mackenzie Canyon, Beaufort Sea. *J Geophys Res Oceans* 103:18447–18458
- Carmack EC, Macdonald RW, Jasper S (2004) Phytoplankton productivity on the Canadian Shelf of the Beaufort Sea. *Mar Ecol Prog Ser* 277:37–50
- Cushing DH, Horwood JW (1994) The growth and death of fish larvae. *J Plankton Res* 16:291–300
- Daase M, Falk-Petersen S, Varpe O, Darnis G, Søreide JE, Wold A, Leu E et al (2013) Timing of reproductive events in the marine copepod *Calanus glacialis*: a pan-Arctic perspective. *Can J Fish Aquat Sci* 70:871–884
- Darnis G, Barber DG, Fortier L (2008) Sea ice and the onshore–offshore gradient in pre-winter zooplankton assemblages in south-eastern Beaufort Sea. *J Mar Syst* 74:994–1011
- Darnis G, Fortier L (2014) Temperature, food and the seasonal vertical migration of key arctic copepods in the thermally stratified Amundsen Gulf (Beaufort Sea, Arctic Ocean). *J Plankton Res* 36:1092–1108
- Darnis G, Robert D, Pomerleau C, Link H, Archambault P, Nelson RJ, Geoffroy M et al (2012) Current state and trends in Canadian Arctic marine ecosystems: II. Heterotrophic food web, pelagic-benthic coupling, and biodiversity. *Clim Change* 115:179–205
- David C, Lange B, Krumpen T, Schaafsma F, van Franeker JA, Flores H (2016) Under-ice distribution of polar cod *Boreogadus saida* in the central Arctic Ocean and their association with sea-ice habitat properties. *Polar Biol* 39:981–994
- Dawson JK (1978) Vertical distribution of *Calanus hyperboreus* in the central Arctic Ocean. *Limnol Oceanogr* 23:950–957
- Demer D, Berger L, Bernasconi M, Bethke E, Boswell K, Chu D, Domokos R et al. (2015) Calibration of acoustic instruments. ICES Cooperative Research Report 133
- Eegeesiak O, Aariak E, Kleist KV (2017) People of the ice bridge: the future of the Pikialasorsuaq. Report of the Pikialasorsuaq Commission, Inuit Circumpolar Council Canada, Ottawa
- Fortier L, Ponton D, Gilbert M (1995) The match/mismatch hypothesis and the feeding success of fish larvae in ice-covered southeastern Hudson Bay. *Mar Ecol Prog Ser* 120:11–27
- Fortier L, Reist JD, Ferguson SH, Archambault P, Matley J, Macdonald RW, Robert D, Darnis G, Geoffroy M, Suzuki K, Falardeau M, MacPhee SA, Majewski AR, Marcoux M, Sawatzky CD, Atchison S, Loseto LL, Grant C, Link H, Asselin NC, Harwood LA, Slavik D, Letcher RJ (2015) Arctic change: impacts on marine ecosystems and contaminants. In: Stern GA, Gaden A (eds) From Science to Policy in the Western and Central Canadian Arctic: An Integrated Regional Impact Study (IRIS) of Climate Change and Modernization. ArcticNet, Québec, pp 200–253
- Fortier M, Fortier L, Michel C, Legendre L (2002) Climatic and biological forcing of the vertical flux of biogenic particles under seasonal Arctic sea ice. *Mar Ecol Prog Ser* 225:1–16
- Francois R, Garrison G (1982) Sound absorption based on ocean measurements. Part II: boric acid contribution and equation for total absorption. *J Acoust Soc Am* 72:1879–1890
- Frank KT (1997) The utility of early life history studies and the challenges of recruitment prediction. In: Chambers RC, Trippel EA (eds) Early life history and recruitment in fish populations. Chapman and Hall, London, pp 495–512
- Gaston AJ, Mallory ML, Gilchrist HG (2012) Populations and trends of Canadian Arctic seabirds. *Polar Biol* 35:1221–1232
- Geoffroy M, Majewski A, LeBlanc M, Gauthier S, Walkusz W, Reist JD, Fortier L (2016) Vertical segregation of age-0 and age-1+ polar cod (*Boreogadus saida*) over the annual cycle in the Canadian Beaufort Sea. *Polar Biol* 39:1023–1037
- Gradinger RR, Bluhm BA (2004) In-situ observations on the distribution and behavior of amphipods and Arctic cod (*Boreogadus saida*) under the sea ice of the High Arctic Canada Basin. *Polar Biol* 27:595–603
- Haecky P, Jonsson S, Andersson A (1998) Influence of sea ice on the composition of the spring phytoplankton bloom in the northern Baltic Sea. *Polar Biol* 20:1–8
- Heide-Jørgensen MP, Burt LM, Hansen RG, Nielsen NH, Rasmussen M, Fossette S, Stern H (2013) The significance of the North Water Polynya to arctic top predators. *Ambio* 42:596–610
- Hirche HJ (1997) Life cycle of the copepod *Calanus hyperboreus* in the Greenland Sea. *Mar Biol* 128:607–618
- Holling CS (1959) Some characteristics of simple types of predation and parasitism. *Can Entomol* 91:385–398
- Horner RA (1985) Ecology of sea ice microalgae. In: Horner RA (ed) Sea ice biota. CRC Press, Cincinnati, pp 83–103
- Hunt GL Jr, Stabeno P, Walters G, Sinclair E, Brodeur RD, Napp JM, Bond NA (2002) Climate change and control of the south-eastern Bering Sea pelagic ecosystem. *Deep Sea Res Part II* 49:5821–5853
- Kahrhu M, Brotas V, Manzano-Sarabia M, Mitchell B (2011) Are phytoplankton blooms occurring earlier in the Arctic? *Glob Change Biol* 17:1733–1739
- Koenker BL, Copeman LA, Laurel B (2018) Impacts of temperature and food availability on the condition of larval Arctic cod (*Boreogadus saida*) and walleye pollock (*Gadus chalcogrammus*). *ICES J Mar Sci* 25:256. <https://doi.org/10.1093/icesjms/fsy052>
- Laurel BJ, Knoth BA, Ryer CH (2016) Growth, mortality, and recruitment signals in age-0 gadids settling in coastal Gulf of Alaska. *ICES J Mar Sci* 73:2227–2237
- Leggett WC, Frank KT (2008) Paradigms in fisheries oceanography. *Oceanogr Mar Biol Annu Rev* 46:331–363
- Leu E, Søreide J, Hessen D, Falk-Petersen S, Berge J (2011) Consequences of changing sea-ice cover for primary and secondary producers in the European Arctic shelf seas: timing, quantity, and quality. *Prog Oceanogr* 90:18–32
- Lønne O, Gulliksen B (1989) Size, age and diet of polar cod, *Boreogadus saida* (Lepechin 1773), in ice covered waters. *Polar Biol* 9:187–191
- Mackenzie KV (1981) Nine-term equation for sound speed in the oceans. *J Acoust Soc Am* 70:807–812
- Madureira LS, Everson I, Murphy EJ (1993) Interpretation of acoustic data at two frequencies to discriminate between Antarctic krill (*Euphausia superba* Dana) and other scatterers. *J Plankton Res* 15:787–802
- Marchese C, Albouy C, Tremblay JE, Dumont D, D’Ortenzio F, Vis-sault S, Bélanger S (2017) Changes in phytoplankton bloom

- phenology over the North Water (NOW) polynya: a response to changing environmental conditions. *Polar Biol* 40:1721–1737
- Martin J, Tremblay JE, Gagnon J, Tremblay G, Lapoussière A, Jose C, Poulin M et al (2010) Prevalence, structure and properties of subsurface chlorophyll maxima in Canadian Arctic waters. *Mar Ecol Prog Ser* 412:69–84
- Melnikov I, Chernova N (2013) Characteristics of under-ice swarming of polar cod *Boreogadus saida* (Gadidae) in the Central Arctic Ocean. *J Ichthyol* 53:7–15
- Michaud J, Fortier L, Rowe P, Ramseier R (1996) Feeding success and survivorship of Arctic cod larvae, *Boreogadus saida*, in the north-east water Polynya (Greenland Sea). *Fish Oceanogr* 5:120–135
- Myers RA (1998) When do environment–recruitment correlations work? *Rev Fish Biol Fish* 8:285–305
- Nakagawa S, Schielzeth H (2013) A general and simple method for obtaining  $R^2$  from generalized linear mixed-effects models. *Methods Ecol Evol* 4:133–142
- National Snow and Ice Data Center (2018) Arctic Sea Ice News and Analysis. <https://nsidc.org/arcticseaicenews/>. Accessed 20 July 2018
- Platt T, White GN III, Zhai L, Sathyendranath S, Roy S (2009) The phenology of phytoplankton blooms: ecosystem indicators from remote sensing. *Ecol Model* 220:3057–3069
- R Core Team (2015) R: A language and environment for statistical computing. R Foundation for Statistical Computing, Vienna
- Ringuette M, Fortier L, Fortier M, Runge JA, Belanger S, Larouche P, Weslawski JM et al (2002) Advanced recruitment and accelerated population development in Arctic calanoid copepods of the North Water. *Deep Sea Res Part II* 49:5081–5099
- Sakshaug E, Slagstad D (1991) Light and productivity of phytoplankton in polar marine ecosystems: a physiological view. *Polar Res* 10:69–86
- Scott JB, Marshall GJ (2010) A step-change in the date of sea-ice breakup in western Hudson Bay. *Arctic* 63:155–164
- Søreide JE, Hop H, Carroll ML, Falk-Petersen S, Hegseth EN (2006) Seasonal food web structures and sympagic–pelagic coupling in the European Arctic revealed by stable isotopes and a two-source food web model. *Prog Oceanogr* 71:59–87
- Søreide JE, Leu E, Berge J, Graeve M, Falk-Petersen S (2010) Timing of blooms, algal food quality and *Calanus glacialis* reproduction and growth in a changing Arctic. *Glob Change Biol* 16:3154–3163
- Stirling I (1980) The biological importance of polynyas in the Canadian Arctic. *Arctic* 33:303–315
- Tremblay JE, Gratton Y, Fauchot J, Price NM (2002) Climatic and oceanic forcing of new, net, and diatom production in the North Water. *Deep Sea Res Part II* 49:4927–4946
- Tremblay JE, Robert D, Varela DE, Lovejoy C, Darnis G, Nelson RJ, Sastri AR (2012) Current state and trends in Canadian Arctic marine ecosystems: I. Primary production *Clim Change* 115:161–178
- Tynan CT, DeMaster DP (1997) Observations and predictions of Arctic climatic change: potential effects on marine mammals. *Arctic* 50:308–322
- Wang Q, Myers PG, Hu XM, Bush ABG (2012) Flow constraints on pathways through the Canadian Arctic Archipelago. *Atmos-Ocean* 50:373–385
- Welch HE, Bergmann MA, Siferd TD, Martin KA, Curtis MF, Crawford RE, Conover RJ et al (1992) Energy flow through the marine ecosystem of the Lancaster Sound Region, Arctic Canada. *Arctic* 45:343–357
- Williams WJ, Carmack EC (2008) Combined effect of wind-forcing and isobath divergence on upwelling at Cape Bathurst, Beaufort Sea. *J Mar Res* 66:645–663
- Wong SN, Gjerdrum C, Morgan KH, Mallory ML (2014) Hotspots in cold seas: the composition, distribution, and abundance of marine birds in the North American Arctic. *J Geophys Res Oceans* 119:1691–1705

**Publisher's Note** Springer Nature remains neutral with regard to jurisdictional claims in published maps and institutional affiliations.